Hydrothermal Aging of Pd/LTA Monolithic Catalyst for Complete CH4 Oxidation

catalysts

MDPI

Article

Hydrothermal Aging of Pd/LTA Monolithic Catalyst for Complete CH_4 Oxidation

Ida Friberg, Aiyong Wang and Louise Olsson *

Chemical Engineering, Competence Centre for Catalysis, Chalmers University of Technology, SE-412 96 Gothenburg, Sweden; ida.friberg@chalmers.se (I.F.); Aiyong@chalmers.se (A.W.)
* Correspondence: louise.olsson@chalmers.se; Tel.: +46-31-772-43-90

Received: 3 April 2020; Accepted: 2 May 2020; Published: 7 May 2020

Abstract: Palladium-based catalysts are known to provide high CH_4 oxidation activity. One drawback for these materials is that they often lose activity in the presence of water vapor due to the formation of surface hydroxyls. It is however possible to improve the water vapor tolerance by using zeolites as support material. In this study, we have investigated Pd supported on thermally stable LTA zeolite with high framework Si/Al ratio (Si/Al = ~44) for CH_4 oxidation and the effect of hydrothermal aging at temperatures up to 900 °C. High and stable CH_4 oxidation activity in the presence of water vapor was observed for Pd/LTA after hydrothermal aging at temperatures ≤ 700 °C. However, aging at temperatures of 800–900 °C resulted in catalyst deactivation. This deactivation was not a result of structural collapse of the LTA zeolite as the LTA zeolite only showed minor changes in surface area, pore volume, and X-ray diffraction pattern after 900 °C aging. We suggest that the deactivation was caused by extensive formation of ion-exchanged Pd^{2+} together with Pd sintering. These two types of Pd species appear to have lower CH_4 oxidation activity and to be more sensitive to water deactivation compared to the well dispersed Pd particles observed on the LTA support prior to the hydrothermal aging. By contrast, Pd/Al_2O_3 was generally sensitive to water vapor no matter of the aging temperature. Although the aging caused extensive Pd sintering in Pd/Al_2O_3, only minor deterioration of the CH_4 oxidation activity was seen. The results herein presented show that Pd/LTA is a promising CH_4 oxidation catalyst, however Pd rearrangement at high temperatures (≥800 °C) is one remaining challenge.

Keywords: Pd/LTA; Pd/Al_2O_3; CH_4 oxidation; hydrothermal aging

1. Introduction

Supported palladium-based catalysts generally express high CH_4 oxidation activity at medium to high temperatures and under conditions free from poisons and deactivating compounds. However, a significant loss of activity is commonly seen after exposure to H_2O and SO_2 [1,2] and after hydrothermal aging [2]. Therefore, deactivation resistant catalysts are required in order to efficiently remove CH_4 from exhaust gas streams in real world applications. The water deactivation at low to medium temperatures, typically <450 °C [3], occurs due to the formation of surface hydroxyl groups which block active PdO sites [3] and/or decreased oxygen transport between Pd and the support material [4,5]. However, at higher temperatures, the water vapor may induce sintering of the Pd and/or the support, hence causing catalyst deactivation by other mechanisms [2,6].

The most well investigated catalytic materials for CH_4 oxidation applications are palladium supported on various metal oxides, most commonly Al_2O_3. Although this type of catalytic materials generally offers high CH_4 conversion under dry conditions, rapid and severe deactivation occurs in the presence of water vapor [2]. Recently, attention has been paid to zeolite supported Pd catalysts due to their potential of providing high tolerance to water vapor [7–10], facilitated regeneration after SO_2

poisoning [7] and to constrain small Pd particles [9,10]. In particular, Pd supported on highly siliceous zeolites [7,8] or on zeolites fully ion-exchanged with alkali metal ions [9,10] show great resistance towards water vapor. This may be a result of limited formation of surface hydroxyls [7,8] and lower tendency to form large Pd agglomerates [9,10] and ion-exchanged Pd^{2+} species [7]. However, many commonly used zeolites, such as BEA and MFI, are known to have poor hydrothermal stability [11–14]. Zeolite SSZ-13 has higher stability and can therefore be operated in a wider temperature window [14,15]. This is one reason for why SSZ-13 has been intensely investigated as catalyst support material during the last decade, above all for SCR applications. However, hydrothermal aging of SSZ-13 at high temperatures (typically > 850 °C) causes structural damage expressed by decreased surface area, pore volume, and changes in X-ray diffraction (XRD) patterns [16]. By contrast, it has recently been demonstrated that the small pore LTA zeolite has extraordinarily good stability with only minor changes in N_2 physisorption and XRD pattern after hydrothermal aging at 900 °C [17,18]. This makes LTA a promising future candidate as a thermally stable zeolite support for heterogenous catalysts. Previously, Pd/LTA has been tested for CH_4 oxidation at temperatures up to 500 °C [19]. However, it is known that high temperature aging in the presence of water facilitates the formation of large Pd agglomerates and ion-exchanged Pd^{2+} species [20,21]. Hence, hydrothermal aging has a huge impact on what type of Pd species are present in Pd/zeolite catalysts which highly impacts the catalytic activity. It is also known that the extent of this Pd rearrangement is highly dependent on the type of zeolite support [20,21]. Therefore, the impact of hydrothermal aging can be expected to differ much depending on the type of zeolite used.

To our knowledge, there are no available studies concerning the impact of hydrothermal aging on Pd/LTA for CH_4 oxidation application. In this study, we aim to unravel how hydrothermal aging impacts the formation of Pd species and the CH_4 oxidation activity of Pd/LTA (monolithic catalyst). This was performed by activity measurement in flow reactor and characterization by N_2 physisorption, XRD, NO adsorption DRIFTS, ICP-SFMS, and STEM. All the results are compared with a Pd/Al_2O_3 reference monolithic catalyst.

2. Results

2.1. Characterization

Note that, in this study, the catalytic reaction of CH_4 oxidation was tested on monolithic catalysts and all characterizations were performed on powder samples. According to the previous research [22], the preparation procedure of monolithic catalyst may have some impact on the property of powder samples. The data in Table 1 show that the hydrothermal aging at 900 °C resulted in about 7% decrease in BET surface area of PdLTA, whereas the corresponding value was about 27% for PdAl. The BET results are in line with earlier measurements on similar samples, for example we observed 542 m^2/g for Cu/LTA treated at 750 °C and 495 m^2/g when it was aged at 900 °C [17]. Moreover, the aging only caused minor changes in pore volume for PdLTA and PdAl (Table 1). The XRD patterns in Figure 1 show that the hydrothermal aging did not result in any large changes in the crystal structure of the LTA zeolite. However, it should be noted that the intensity of all LTA peaks increased slightly which indicates additional crystallization of the LTA zeolite upon 900 °C hydrothermal aging. For PdAl, small changes in diffraction peaks corresponding to the support material can be noted, however it can be concluded that support material mainly consisted of γ-Al_2O_3 also after the hydrothermal aging [23]. The N_2 physisorption and XRD results indicate that the LTA zeolite is extraordinarily resistant towards structural changes upon hydrothermal aging, which agrees well with our previous report [17]. However, Al_2O_3 expressed also high thermal stability.

Table 1. Pd content and Si/Al molar ratio measured by ICP-SFMS together with BET surface area, t-plot micropore volume and BJH pore volume of degreened and 900 °C aged samples

	Pd Content (wt %)	Si/Al Molar Ratio (-)		BET Surface Area (m^2/g)	Micropore Volume (t-plot, cm^3/g)	Pore Volume (BJH, cm^3/g)
PdLTA *(Pd/H-LTA)*	2.12	44	Degreened (600 °C)	500	0.18	0.35
			Aged (900 °C)	464	0.17	0.32
PdAl *(Pd/γ-Al_2O_3)*	2.21	-	Degreened (600 °C)	170	0.00	0.50
			Aged (900 °C)	123	0.00	0.44

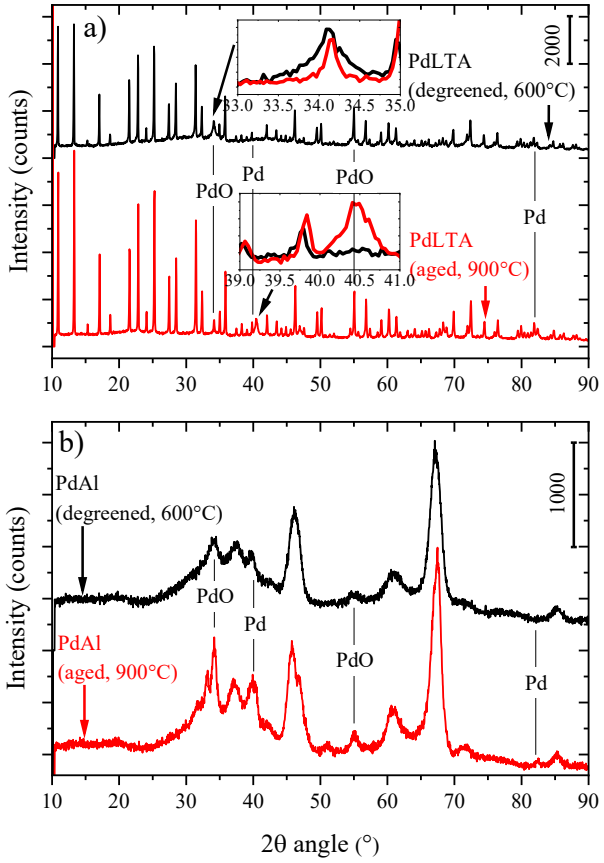

Figure 1. X-ray diffraction (XRD) patters of (**a**) PdLTA and (**b**) PdAl. Black lines represent degreened sample and red lines show the samples after hydrothermal aging at 900 °C.

The XRD patterns in Figure 1 also reveal information about the Pd particles. For PdAl a clear growth and sharpening of the PdO peaks at 2θ = 34° and 2θ = 55° as well for the peak corresponding to metallic Pd at 2θ = 40° can be seen [23]. This infers sintering and formation of larger Pd particles upon aging of PdAl. The diffractograms of degreened and aged PdLTA do not show any significant differences of the PdO peaks at 2θ of 55°, where the PdO peak at 2θ of 34° become sharper after 900 °C aging without a clear intensity increase. However, the appearance of a peak a 2θ = 40.4° indicates formation of an additional crystalline Pd phase upon aging of PdLTA [23] which may suggest Pd sintering into metallic Pd particles.

Further information of the Pd particles can be retrieved from the STEM images in Figure 2. The degreened PdLTA sample contained Pd particles with diameters evenly spread within the interval of 1–20 nm in addition to a low number of larger Pd agglomerates. After aging the Pd particle range was about 10–35 nm also together with a low number of larger particles as well as smaller particles. Moreover, according to the NO-DRIFTS profiles discussed in next paragraph, it is suggested that some of the Pd particles were converted to ion-exchanged Pd ions upon aging, which were not visible in the STEM images. PdAl expressed clear Pd rearrangement upon hydrothermal aging. The degreened

PdAl exhibited well dispersed Pd particles in the range 2–6 nm. After 900 °C hydrothermal aging, the small Pd particles were absent and larger agglomerates of around 20–60 nm had been formed. Hence, the STEM images clearly show extensive Pd sintering of PdAl upon aging which agrees well with the XRD results. The STEM images also expressed a trend of Pd sintering in PdLTA, is supported by the growth of the crystalline Pd peak in the XRD patterns. Moreover, SEM images of monolithic catalysts are shown in Figure S1 to elucidate the distribution of the washcoat. It is clear that our washcoat procedure can distribute the catalyst well on the wall of the monolith. The apparent presence of small amounts of Pd in the cordierite in the EDX maps is due to a detector artefact. The high Al concentration in the cordierite results in a so called double (or sum) peak at 3 keV in the spectrum which partially overlaps with, and is of the same magnitude as, the Pd peak used in the generation of the EDX map. A complete separation of these peaks was not possible.

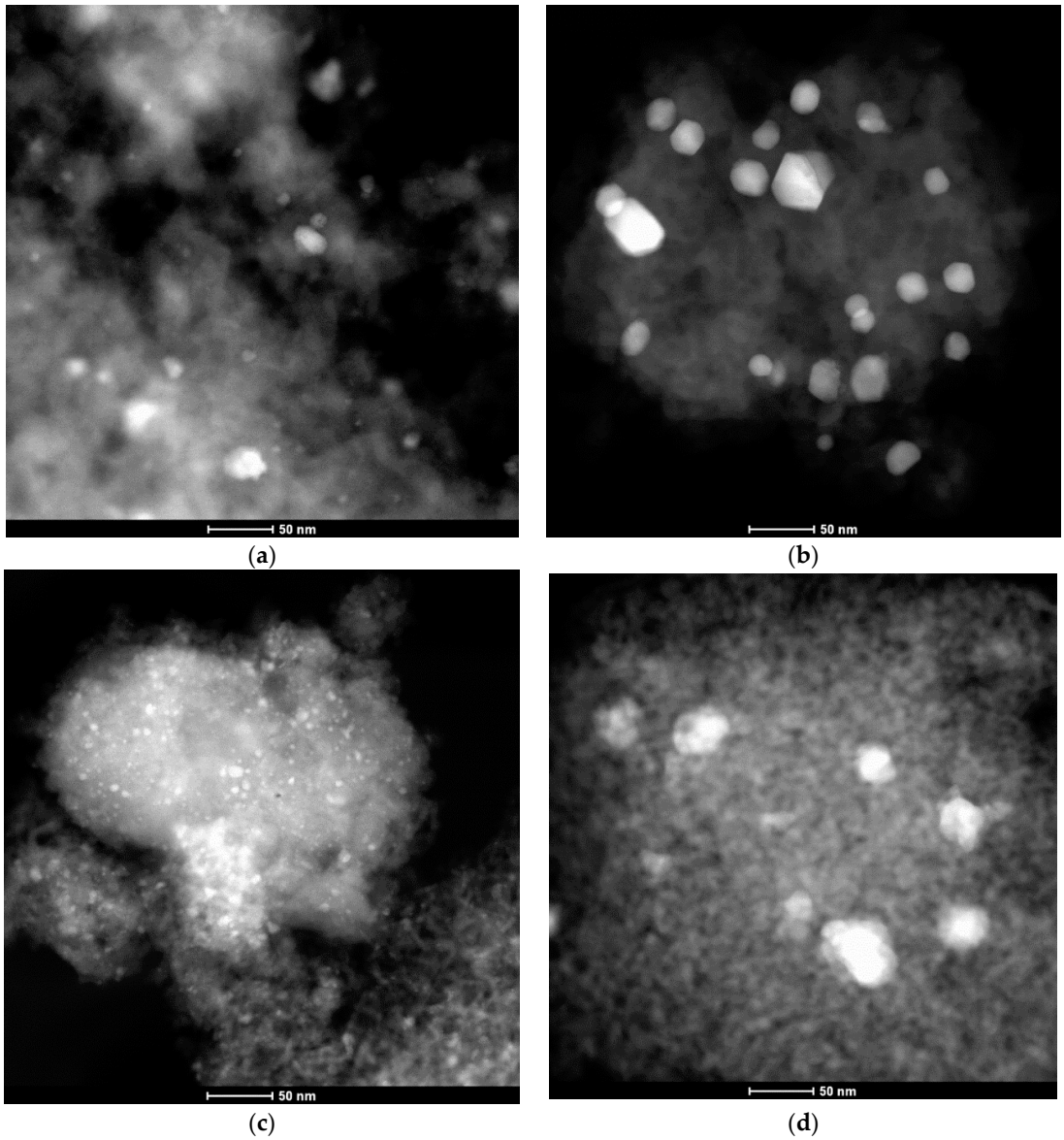

Figure 2. Scanning transmission electron microscopy (STEM) images of (**a**) degreened PdLTA, (**b**) 900 °C aged PdLTA, (**c**) degreened PdAl, and (**d**) 900 °C aged PdAl.

Upon NO exposure of Pd/zeolite materials, nitrosyl groups will be formed on the ion-exchanged Pd^{2+} species and these groups can easily be identified with IR absorbance techniques. Therefore, NO adsorption was combined with DRIFTS to identify monodispersed Pd species in PdLTA. It should

be noted that Pd particles generally adsorb very little NO [21,24,25]. Nitrosyl groups on Pd^{2+} typically absorb IR radiation with wave numbers of 1800–1881 cm^{-1} [7,21,26–29]. It is clear from the spectra in Figure 3a that the degreened and 900 °C aged PdLTA sample expressed largest difference in IR absorbance in this region. The intense peaks of 900 °C aged PdLTA at 1864 and 1814 cm^{-1} were only weakly distinguishable for degreened PdLTA. Hence, it can be concluded that parts of the Pd particles that were present in PdLTA after degreening at 600 °C transformed into isolated Pd species during 900 °C hydrothermal aging. The peak at around 2165 cm^{-1} is assigned to NO^+ adsorbed on acid Brønsted sites in the zeolite framework. This surface species has previously been reported to absorb IR in the region of 2220–2128 cm^{-1} for different types of zeolites [7,26–28,30,31]. The intensity of IR absorbance in this region significantly decreased for PdLTA after 900 °C hydrothermal aging. The fact that 900 °C aging caused simultaneous growth of the 1864/1814 cm^{-1} peaks and decrease of the 2165 cm^{-1} peak indicates that many acid Brønsted sites were blocked from NO adsorption by Pd^{2+} ions. Moreover, the absorbance peaks in the region around 1570–1630 cm^{-1} are assigned to surface nitrates [7,26,32,33].

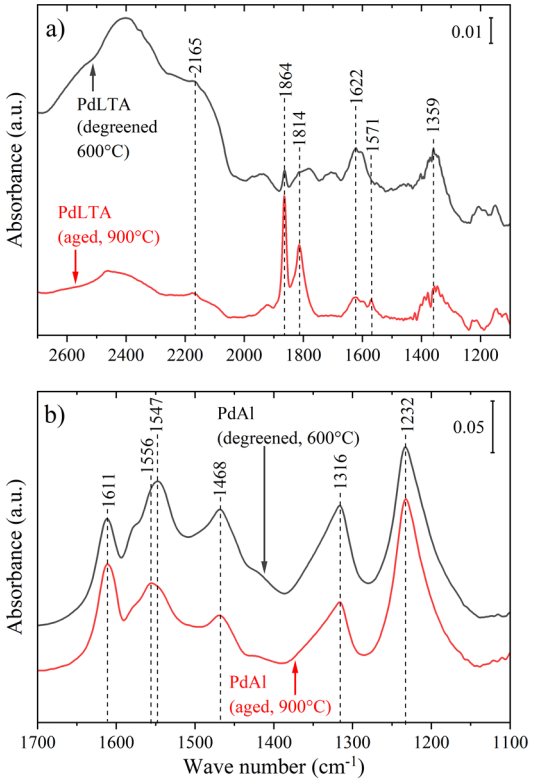

Figure 3. Diffuse reflectance infrared Fourier transform spectroscopy (DRIFTS) spectra collected at 80 °C after 60 min exposure to 200 ppm NO of (**a**) PdLTA and (**b**) PdAl. The spectra are corrected with the sample background which was acquired at 80 °C in Ar prior to the NO exposure. Black lines represent samples degreened at 600 °C and red lines show samples aged for 8 h in O_2 and H_2O at 900 °C (see Section 3.2.4).

The absorbance spectra of degreened and 900 °C aged PdAl are rather similar, as shown in Figure 3b. Note that no major bands were observed in the region of 1700–2700 cm^{-1}, and this region is therefore not shown for PdAl. The NO adsorption ability is generally low on Pd particles [21,24,25], thus the spectra of PdAl mostly show the NO adsorption on the Al_2O_3 support. The IR absorbance in the wave number region 1611–1547 cm^{-1} and 1316 cm^{-1} is assigned to surface nitrates, whereas the absorbance at the lower wave number 1232 cm^{-1} corresponds to surface nitrites [34]. The fact that the NO adsorption properties of the alumina did not change much after the hydrothermal aging at 900 °C may be an indication of that the alumina was rather insensitive to the harsh aging conditions.

2.2. Catalytic Activity of Degreened and Aged Samples

The catalytic activity results from isothermal CH_4 oxidation test after degreening and aging at 700, 800, and 900 °C are displayed in Figure 4. After degreening at 600 °C, PdLTA expressed high and stable activity in the wet reaction mixture (Figure 4a). Aging at 700 °C resulted in slightly less stable CH_4 oxidation activity over time, whereas PdLTA aged at 800 °C and 900 °C were rather quickly deactivated in the wet reaction mixture. Interestingly, the activity was rather high (90% conversion) initially after aging at 800 °C and pre-treatment. However, after 9 h of exposure to the wet gas feed, the conversion was only 30%. The similar trend was seen after aging at 900 °C, as the initial conversion was 50% which dropped to 16% after 9 h. Thus, the time for stabilization for PdLTA aged at 800 °C and 900 °C, is very different, where the 900 °C PdLTA is fast to reach the stable level, although conversion is very low. This phenomenon is possibly due to the change of Pd nature during aging. From NO-DRIFTS analysis (Figure 3), it was found that the amount of ion-exchanged Pd species increased after aging. Ion-exchanged Pd are very sensitive to water, which has been observed for Pd/zeolites used as passive NOx adsorbers [35]. The larger amount of Pd^{2+}, which are sensitive to water, in the 900 °C sample, can explain why the conversion drops very fast and to a low value. Hence, it appears that PdLTA was not necessarily very deactivated after the high temperature aging, but the sensitivity to water vapor was significantly increased. By contrast, PdAl showed a steady decrease in CH_4 conversion during 9 h of exposure to the wet gas conditions for all aged samples (Figure 4b). This drop of activity over time is typical for Al_2O_3 supported Pd [2] and occurs due to the accumulation of surface hydroxyls which blocks active PdO sites [3] and/or decrease the oxygen exchange between the support material and the Pd [4,5]. The catalytic activity of PdAl was only slightly deteriorated after 900 °C aging, thus PdAl was generally rather insensitive to the hydrothermal aging in terms of CH_4 oxidation activity in the presence of water vapor. However, a large disadvantage with PdAl is the large sensitivity to water vapor.

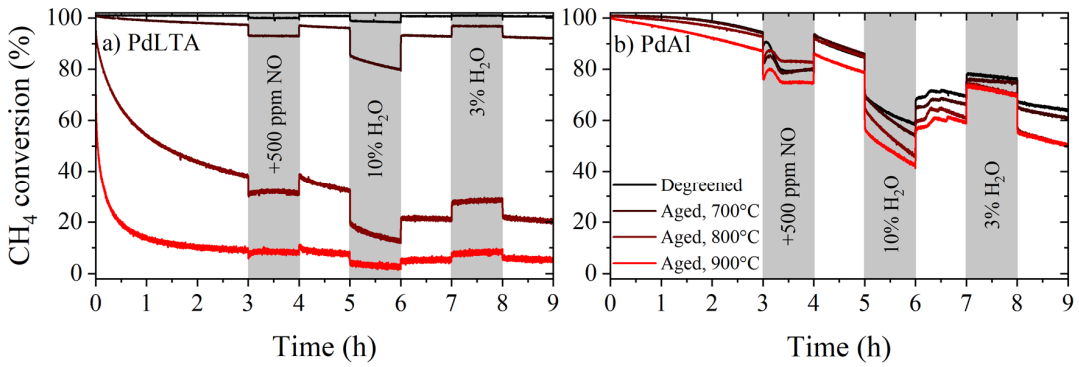

Figure 4. Isothermal CH_4 oxidation activity test at 450 °C for (**a**) PdLTA and (**b**) PdAl that had been degreened or aged at 700, 800, or 900 °C. White areas correspond to wet reaction mixture (500 ppm CH_4, 8% O_2, and 5% H_2O). Grey areas represent wet reaction mixture modified according to the text in each grey box.

After 3 h of activity testing, 500 ppm NO was added to the wet reaction mixture. This resulted in a decreased conversion for PdLTA, especially after aging at 700 °C and 800 °C. Sadokhina et al. [36] addressed this phenomenon to the formation of blocking surface compounds as NO is present in the gas feed. In agreement to what we have observed previously [7], the slow and accumulative water deactivation over time paused during the time NO was present. Once NO was removed from the gas feed, the CH_4 oxidation activity returned to the same level as before the introduction of NO. PdAl exhibited the same response to the addition of NO.

When the water vapor level was increased to 10% after 5 h of testing, the CH_4 oxidation activity for both the samples decreased immediately which most likely was due to quick formation of surface hydroxyls [7,37]. Once the water vapor concentration was changed back to 5%, or to the even lower

level of 3%, the CH_4 oxidation activity rapidly increased again. For PdLTA, the response to changed water vapor concentration was particularly pronounced after aging at 700 °C and 800 °C. It is possible that the activity of PdLTA already was too low after aging at 900 °C and that the response to the water vapor concentration therefore was mild. For PdAl, the response to the water vapor concentration was only slightly dependent on the aging conditions.

After finalizing the isothermal activity test, seen in Figure 4, the temperature was decreased to 150 °C in wet reaction mixture. Thereafter the temperature was ramped 5 °C/min to 700 °C in wet reaction mixture. The concurrently measured CH_4 conversion during the latter mentioned temperature ramp is displayed in Figure 5 and the corresponding temperature of 50% CH_4 conversion ($T_{50\%}$) is shown in Figure 6. After degreening, $T_{50\%}$ was 41 °C lower for PdLTA compared to PdAl. After aging at 700 °C this difference was 20 °C, i.e., slightly smaller. Aging at higher temperatures resulted in higher $T_{50\%}$ for PdLTA compared to PdAl, more precisely 68 °C and 118 °C higher after aging at 800 °C and 900 °C, respectively.

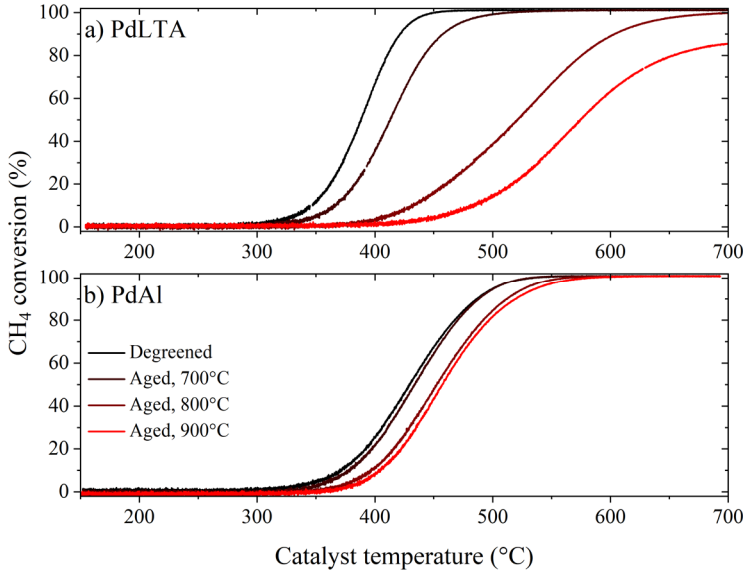

Figure 5. Temperature programmed CH_4 oxidation activity test during heating 5 °C/min for (**a**) PdLTA and (**b**) PdAl, which had been degreened or aged at 700, 800, or 900 °C. Note that this activity test followed directly after the isothermal activity in Figure 4 (without pre-treatment in between). The entire test was performed in wet reaction mixture (500 ppm CH_4, 8% O_2, and 5% H_2O).

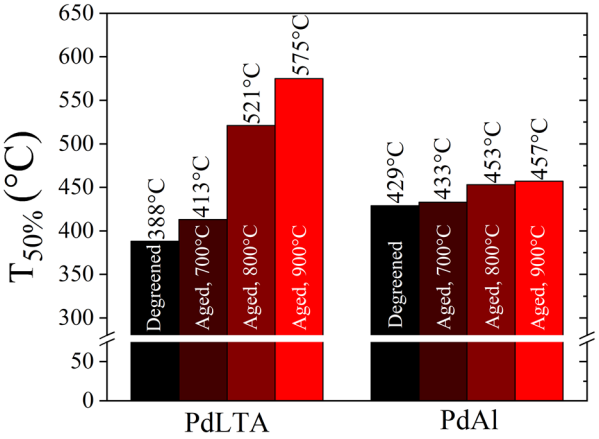

Figure 6. Temperature of 50% CH_4 conversion ($T_{50\%}$) of the temperature programmed activity test in Figure 5.

To summarize the activity tests, PdLTA expressed both high CH_4 oxidation activity and high tolerance to water vapor after degreening at 600 °C and aging at 700 °C. Hence, PdLTA shows excellent CH_4 oxidation catalyst properties when treated at temperatures ≤700 °C. However, hydrothermal aging at the higher temperatures of 800 °C and 900 °C caused deactivation and significantly decreased the resistance to water deactivation. Characterization by XRD and N_2 physisorption indicated that this was not caused by zeolite structure collapse, as only minor changes were obtained in the crystallinity, BET area, and pore volume after 900 °C aging. On the other hand, it was seen from the NO-DRIFTS, STEM, and XRD that 900 °C hydrothermal aging resulted in extensive formation of ion-exchanged Pd^{2+} species in addition to Pd sintering, a phenomenon which appears to be enhanced by treatment at high temperature. A similar behavior of Pd/H-SSZ-13 after hydrothermal aging at 750 °C has been reported previously [21]. However, with results herein, we can link these structural rearrangements of the Pd to decreased CH_4 oxidation activity. Agglomeration of Pd and formation of ion-exchanged Pd^{2+} species have been reported to be facilitated at high temperatures, in the presence of water vapor [21] and for Pd supported on zeolites with larger pore openings [20,38]. Therefore, the small pore size of LTA zeolite is probably beneficial for CH_4 oxidation catalyst support, as zeolites with large pore sizes may enhance the mobility of the Pd and probably result in formation of ion-exchanged Pd species and large Pd particles more easily.

3. Materials and Methods

3.1. Catalyst Preparation

Two catalyst samples were prepared, Pd/H-LTA (PdLTA) and Pd/γ-Al_2O_3 (PdAl). The Si/Al-ratio of the H-LTA zeolite was 44 (measured by ICP-SFMS performed by ALS Scandinavia AB) and it was synthesized according to the procedure described in our previous publication [17]. For the γ-Al_2O_3 support, Puralox SBa 200 calcined at 700 °C for 2 h was used. The samples contained 2 wt % of Pd which was deposited onto the support materials by incipient wetness impregnation with $Pd(NO_3)_2$ solution (Alfa Aesar, Kandel, Germany). After impregnation with $Pd(NO_3)_2$ solution, the samples were dried at 80 °C and calcined for 2 h at 550 °C.

The catalytic activity measurements were conducted using washcoated cordierite monoliths (L= 20 mm, D = 15 mm, 400 cpsi). The washcoating was performed by dipping the monoliths in a washcoat slurry consisting of 10 wt % solids (95 wt % catalyst powder, 5 wt. % boehmite binder, Sasol Dispersal P2, Brunsbüttel, Germany) and 90 wt % liquids (50 wt % ethanol, 50 wt % deionized water). This was followed by drying in a 90 °C air flow. The monoliths were constantly rotated while being dried in order to distribute the washcoat evenly in the channels. The final monoliths contained 250 ± 5 mg washcoat and were calcined for 2 min in an air flow of 500 °C and for 2 h at 500 °C in a muffle oven.

3.2. Catalytic Activity Tests and Aging

Degreening, pre-treatment, aging, and catalytic activity testing were performed in a flow reactor, which is described in our previous publication [7]. Briefly, the monolith was inserted in quartz tube surrounded by a heating coil and insulation. The heating was controlled and measured by an Eurotherm system and two thermocouples located centrally and slightly upstream of the monolith. The gases were dosed by multiple Bronkhorst mass flow controllers and the water was controlled by a Bronkhorst CEM (Controlled Evaporation Mixing, Ruurlo, Netherlands) system. A Fourier Transform Infrared (FTIR) spectrometer (MKS MultiGas 2030 HS FTIR, provided by MKS instruments, Andover, MA, USA) was used to measure the outlet gases. The individual gases were balanced with Ar to give a total flow of 0.8 L/min (13,600 h^{-1}). The catalytic activity test was typically tested in a gas mixture consisting of 500 ppm CH_4, 8% O_2, and 5% H_2O which will be referred to as "wet reaction mixture".

3.2.1. Degreening and Pre-Treatment

All washcoated monolith samples were degreened and pre-treated prior to the catalytic activity test. The degreening procedure is summarized in the following steps:

1. 2% H_2 at 500 °C (30 min)
2. Wet reaction mixture at 600 °C (60 min)
3. 2% H_2 and 5% H_2O at 600 °C (20 min)
4. Wet reaction mixture at 600 °C (60 min)

The subsequent pre-treatment was performed in the following steps:

1. 2% H_2 at 600 °C (30 min)
2. 8% O_2 at 600 °C (30 min)
3. Cooling in 8% O_2 to 250 °C

Note that after aging at 700, 800, and 900 °C, the pre-treatment was performed at 700 °C instead of 600 °C (i.e., Step 1–2 above). The pre-treatment is illustrated in Figure 7.

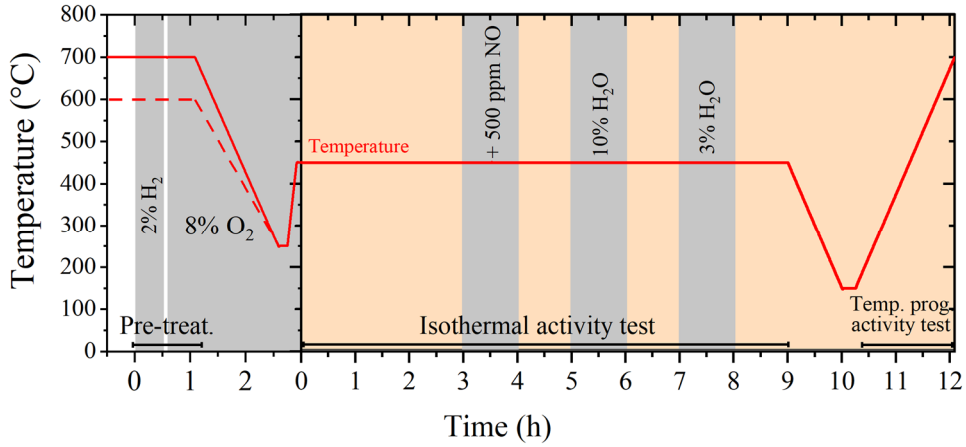

Figure 7. Illustration of the experimental procedure for the pre-treatment, isothermal activity test and the temperature programmed activity test. Note that orange areas correspond to wet reaction mixture. Modifications of the wet reaction mixture during the activity test can be seen in the figure (grey areas).

3.2.2. Catalytic Activity Tests

The catalytic activity was tested under wet conditions after the degreening and after each of the hydrothermal aging. Note that irrespective of previous treatment the catalytic activity always followed directly after the pre-treatment (Section 3.2.1.) in order to minimize the amount of adsorbed surface species and to start with an oxidized catalyst. The activity test is illustrated in Figure 7 and is described in the following steps:

1. Heating in 8% O_2 to 450 °C
2. Wet reaction mixture at 450 °C (3 h)
3. Wet reaction mixture + 500 ppm NO at 450 °C (1 h)
4. Wet reaction mixture at 450 °C (1 h)
5. Wet reaction mixture but with 10% H_2O at 450 °C (1 h)
6. Wet reaction mixture at 450 °C (1 h)
7. Wet reaction mixture but with 3% H_2O at 450 °C (1 h)
8. Wet reaction mixture at 450 °C (1 h)
9. Cooling to 150 °C in wet reaction mixture
10. Heating to 700 °C in wet reaction mixture (5 °C/min)

Step 2–8 in the list above represent the isothermal activity test and Step 10 is the temperature programmed activity test. Note that sudden spikes in the CH_4 concentration data were observed due to water condensation and have been removed in the figures. This has no influence on the interpretation of the results and the original figures can be found in the Supplementary Materials.

3.2.3. Hydrothermal Aging

The monolith samples were aged for 8 h in 8% O_2 and 5% H_2O at 700, 800, and 900 °C. After each aging step, the samples were pre-treated (Section 3.2.1) followed by catalytic activity tests (Section 3.2.2). Thus, the entire test sequence for each sample can be summarized accordingly:

1. Degreening
2. Pre-treatment 600 °C
3. Activity test
4. Aging 700 °C
5. Pre-treatment 700 °C
6. Activity test
7. Aging 800 °C
8. Pre-treatment 700 °C
9. Activity test
10. Aging 900 °C
11. Pre-treatment 700 °C
12. Activity test

3.2.4. Degreening and Hydrothermal Aging of Catalyst Powder for Characterization

Catalyst powder intended for characterization was put in a ceramic crucible boat inside the reactor tube. The powder was then treated under similar conditions as described above. In detail, one part of the powder was degreened according to the procedure in Section 3.2.1, this was followed by cooling to 100 °C in 5% H_2O and 8% O_2 and to room temperature in in 8% O_2. The second part of the powder was first degreened and cooled in the same way, it was thereafter aged for 8 h at 900 °C in 5% H_2O and 8% O_2. The powder was subsequently cooled to 100 °C in 5% H_2O and 8% O_2 and to room temperature in 8% O_2. Thus, the characterization powder was expected to contain surface hydroxyl groups and to be oxidized.

3.3. Characterization

All characterization was performed on powder which had been only degreened or both degreened and 900 °C hydrothermally aged powder (Section 3.2.4). The BET surface area and t-plot micropore volume were measured by N_2 physisorption using a TriStar 3000 instrument (from Micromeritics, GA, USA). The samples were degassed in N_2 at 240 °C for 4 h prior to the measurements. The Pd particles were studied with scanning transmission electron microscopy (STEM) using a FEI Titan 80–300 microscope (Hillsboro, OR, USA) operated at 300 kV. The Pd particle size was estimated from the acquired images. Information of crystal structure was retrieved from powder X-ray diffraction (XRD) using a BrukerAXS D8 advance diffractometer (Billerica, MA, USA)) operated at 40 kV/40 mA with a nickel-filtered Cu Kα source (λ = 1.5418 Å). Diffraction data was recorded in the 2θ interval of 10–90° with steps of 0.02°.

The samples were further characterized by diffuse reflectance infrared Fourier transform spectroscopy (DRIFTS) by studying the surface compounds formed during NO adsorption. This was performed with a Vertex 70 spectrometer (Billerica, MA, USA) equipped with an MCT detector. The sample was loaded into a high temperature reaction chamber (Harrick Praying Mantis, Ossining, NY, USA) equipped with CaF_2 windows. The individual gases were balanced with Ar and dosed by

multiple mass flow controllers (Bronkhorst, Ruurlo, Netherlands). A total flow of 0.1 L/min was used. Prior to the NO adsorption, the samples were pre-treated in cell at 550 °C in 2% H_2 for 30 min and in 8% O_2 for 30 min. The samples were thereafter cooled to 80 °C in 8% O_2 and subsequently flushed in Ar for 1.5 h at 80 °C. The sample background was acquired in the end of this step, i.e., in pure Ar at 80 °C. The NO adsorption was thereafter conducted in 0.02 % NO at 80 °C for 1 h. The spectra herein presented were recorded in the end of this step and are background corrected.

4. Conclusions

Palladium supported on H-LTA was tested for CH_4 oxidation in the presence of water vapor before and after hydrothermal aging at temperatures up to 900 °C. PdLTA expressed excellent CH_4 oxidation activity after treatment at temperatures ≤ 700 °C. Particularly noteworthy was the high tolerance to water vapor, i.e., almost no water deactivation over time. Hydrothermal aging of PdLTA at higher temperatures of 800–900 °C resulted in extensive formation of isolated Pd species in addition to Pd sintering. This decreased the CH_4 oxidation activity and made PdLTA significantly more sensitive to water vapor. Interestingly, the surface area, pore volume and crystallinity of the LTA only changed slightly during aging at 900 °C, meaning that the LTA zeolite has high thermal stability. Hence, we suggest that the Pd rearrangement of PdLTA was responsible for the deactivation upon aging and not structural changes of the LTA zeolite. By comparison with PdAl, extensive Pd sintering was seen after 900 °C hydrothermal aging but this did not result in any major changes in the catalytic performance or CH_4 oxidation activity. However, PdAl was sensitive to water vapor due to accumulative hydroxyl accumulation, no matter if it was degreened only or hydrothermally aged. The results herein presented show that PdLTA is a promising catalyst for CH_4 oxidation with high and stable CH_4 oxidation when treated at temperatures up to 700 °C. However, operation at higher temperatures is challenging due to deactivating Pd rearrangement, despite the high thermal stability of the LTA zeolite.

Supplementary Materials: The following are available online at http://www.mdpi.com/2073-4344/10/5/517/s1, Figure S1: SEM images of PdAl and PdLTA; Figure S2: Original figure, without removal of CH_4 spikes due to water condensation, corresponding to Figure 4; Figure S3: Original figure, without removal of CH_4 spikes due to water condensation, corresponding to Figure 5.

Author Contributions: Conceptualization, I.F., A.W., and L.O.; Data curation, I.F. and A.W.; Formal analysis, I.F. and A.W.; Methodology, I.F., A.W., and L.O.; Supervision, L.O.; Writing—original draft, I.F.; Writing—review and editing, I.F., A.W., and L.O. All authors have read and agreed to the published version of the manuscript.

Funding: This research was funded by Swedish Research Council (grant number 642-2014-5733).

Conflicts of Interest: The authors declare no conflict of interest.

References

1. Gelin, P.; Primet, M. Complete oxidation of methane at low temperature over noble metal based catalysts: A review. *Appl. Catal. B Environ.* **2002**, *39*, 1–37. [CrossRef]
2. Gholami, R.; Alyani, M.; Smith, K.J. Deactivation of Pd catalysts by water during low temperature methane oxidation relevant to natural gas vehicle converters. *Catalysts* **2015**, *5*, 561–594. [CrossRef]
3. Burch, R.; Urbano, F.J.; Loader, P.K. Methane combustion over palladium catalysts: The effect of carbon dioxide and water on activity. *Appl. Catal. A Gen.* **1995**, *123*, 173–184. [CrossRef]
4. Schwartz, W.R.; Ciuparu, D.; Pfefferle, L.D. Combustion of methane over palladium-based catalysts: Catalytic deactivation and role of the support. *J. Phys. Chem. C* **2012**, *116*, 8587–8593. [CrossRef]
5. Schwartz, W.R.; Pfefferle, L.D. Combustion of methane over palladium-based catalysts: Support interactions. *J. Phys. Chem. C* **2012**, *116*, 8571–8578. [CrossRef]
6. Bartholomew, C.H. Mechanisms of catalyst deactivation. *Appl. Catal. A Gen.* **2001**, *212*, 17–60. [CrossRef]
7. Friberg, I.; Sadokhina, N.; Olsson, L. The effect of Si/Al ratio of zeolite supported Pd for complete CH4 oxidation in the presence of water vapor and SO_2. *Appl. Catal. B Environ.* **2019**, *250*, 117–131. [CrossRef]
8. Okumura, K.; Shinohara, E.; Niwa, M. Pd loaded on high silica beta support active for the total oxidation of diluted methane in the presence of water vapor. *Catal. Today* **2006**, *117*, 577–583. [CrossRef]

9. Petrov, A.W.; Ferri, D.; Krocher, O.; Van Bokhoven, J.A. Design of Stable Palladium-Based Zeolite Catalysts for Complete Methane Oxidation by Postsynthesis Zeolite Modification. *ASC Catal.* **2019**, *9*, 2303–2312. [CrossRef]
10. Petrov, A.W.; Ferri, D.; Krumeich, F.; Nachtegaal, M.; Van Bokhoven, J.A.; Kröcher, O. Stable complete methane oxidation over palladium based zeolite catalysts. *Nat. Commun.* **2018**, *9*, 2545. [CrossRef]
11. Petrov, A.; Ferri, D.; Tarik, M.; Krocher, O.; Bokhoven, J. Deactivation Aspects of Methane Oxidation Catalysts Based on Palladium and ZSM-5. *Top. Catal.* **2017**, *60*, 123–130. [CrossRef]
12. Liu, S.-b.; Wu, J.-F.; Ma, L.-J.; Tsai, T.-C.; Wang, I. On the thermal stability of zeolite beta. *J. Catal.* **1991**, *132*, 432–439. [CrossRef]
13. Ding, L.; Zheng, Y.; Hong, Y.; Ring, Z. Effect of particle size on the hydrothermal stability of zeolite beta. *Microporous Mesoporous Mat.* **2007**, *101*, 432–439. [CrossRef]
14. Kwak, J.H.; Tran, D.; Burton, S.D.; Szanyi, J.; Lee, J.H.; Peden, C.H.F. Effects of hydrothermal aging on NH3-SCR reaction over Cu/zeolites. *J. Catal.* **2012**, *287*, 203–209. [CrossRef]
15. Blakeman, P.G.; Burkholder, E.M.; Chen, H.-Y.; Collier, J.E.; Fedeyko, J.M.; Jobson, H.; Rajaram, R.R. The role of pore size on the thermal stability of zeolite supported Cu SCR catalysts. *Catal. Today* **2014**, *231*, 56–63. [CrossRef]
16. Leistner, K.; Kumar, A.; Kamasamudram, K.; Olsson, L. Mechanistic study of hydrothermally aged Cu/SSZ-13 catalysts for ammonia-SCR. *Catal. Today* **2018**, *307*, 55–64. [CrossRef]
17. Wang, A.Y.; Arora, P.; Bernin, D.; Kumar, A.; Kamasamudram, K.; Olsson, L. Investigation of the robust hydrothermal stability of Cu/LTA for NH3-SCR reaction. *Appl. Catal. B Environ.* **2019**, *246*, 242–253. [CrossRef]
18. Ryu, T.; Ahn, N.H.; Seo, S.; Cho, J.; Kim, H.; Jo, D.; Park, G.T.; Kim, P.S.; Kim, C.H.; Bruce, E.L.; et al. Fully Copper-Exchanged High-Silica LTA Zeolites as Unrivaled Hydrothermally Stable NH3-SCR Catalysts. *Angew. Chem. Int. Ed.* **2017**, *56*, 3256–3260. [CrossRef]
19. Lim, J.B.; Jo, D.; Hong, S.B. Palladium-exchanged small-pore zeolites with different cage systems as methane combustion catalysts. *Appl. Catal. B Environ.* **2017**, *219*, 155–162. [CrossRef]
20. Lee, J.; Ryou, Y.; Hwang, S.; Kim, Y.; Cho, S.J.; Lee, H.; Kim, C.H.; Kim, D.H. Comparative study of the mobility of Pd species in SSZ-13 and ZSM-5, and its implication for their activity as passive NOx adsorbers (PNAs) after hydro-thermal aging. *Catal. Sci. Technol.* **2019**, *9*, 163–173. [CrossRef]
21. Ryou, Y.; Lee, J.; Cho, S.J.; Lee, H.; Kim, C.H.; Kim, D.H. Activation of Pd/SSZ-13 catalyst by hydrothermal aging treatment in passive NO adsorption performance at low temperature for cold start application. *Appl. Catal. B Environ.* **2017**, *212*, 140–149. [CrossRef]
22. Hernandez-Garrido, J.C.; Gomez, D.M.; Gaona, D.; Vidal, H.; Gatica, J.M.; Sanz, O.; Rebled, J.M.; Peiro, F.; Calvino, J.J. Combined (S)TEM-FIB Insight into the Influence of the Preparation Method on the Final Surface Structure of a Co_3O_4/La-Modified-CeO_2 Washcoated Monolithic Catalyst. *J. Phys. Chem. C* **2013**, *117*, 13028–13036. [CrossRef]
23. Thevenin, P.O.; Pocoroba, E.; Pettersson, L.J.; Karhu, H.; Vayrynen, I.J.; Jaras, S.G. Characterization and activity of supported palladium combustion catalysts. *J. Catal.* **2002**, *207*, 139–149. [CrossRef]
24. Ogura, M.; Hayashi, M.; Kage, S.; Matsukata, M.; Kikuchi, E. Determination of active palladium species in ZSM-5 zeolite for selective reduction of nitric oxide with methane. *Appl. Catal. B Environ.* **1999**, *23*, 247–257. [CrossRef]
25. Watson, J.M.; Ozkan, U.S. Adsorption characteristics of sol-gel Gd-Pd/TiO_2 catalysts in reduction of nitric oxide with CH4: DRIFTS and TPD. *J. Catal.* **2002**, *210*, 295–312. [CrossRef]
26. Chakarova, K.; Ivanova, E.; Hadjiivanov, K.; Klissurski, D.; Knozinger, H. Co-ordination chemistry of palladium cations in Pd-H-ZSM-5 as revealed by FTIR spectra of adsorbed and co-adsorbed probe molecules (CO and NO). *Phys. Chem. Chem. Phys.* **2004**, *6*, 3702–3709. [CrossRef]
27. Chen, H.Y.; Collier, J.E.; Liu, D.X.; Mantarosie, L.; Duran-Martin, D.; Novak, V.; Rajaram, R.R.; Thompsett, D. Low Temperature NO Storage of Zeolite Supported Pd for Low Temperature Diesel Engine Emission Control. *Catal. Lett.* **2016**, *146*, 1706–1711. [CrossRef]
28. Lonyi, F.; Solt, H.E.; Valyon, J.; Decolatti, H.; Gutierrez, L.B.; Miro, E. An operando DRIFTS study of the active sites and the active intermediates of the NO-SCR reaction by methane over In,H- and In,Pd,H-zeolite catalysts. *Appl. Catal. B Environ.* **2010**, *100*, 133–142. [CrossRef]

29. Pommier, B.; Gelin, P. On the nature of Pd species formed upon exchange of H-ZSM5 with Pd(NH3)(4)(2+) and calcination in O-2. *Phys. Chem. Chem. Phys.* **1999**, *1*, 1665–1672. [CrossRef]
30. Loiland, J.A.; Lobo, R.F. Oxidation of zeolite acid sites in NO/O-2 mixtures and the catalytic properties of the new site in NO oxidation. *J. Catal.* **2015**, *325*, 68–78. [CrossRef]
31. Hadjiivanov, K.; Saussey, J.; Freysz, J.L.; Lavalley, J.C. FT-IR study of NO+O-2 co-adsorption on H-ZSM-5: Re-assignment of the 2133 cm(-1) band to NO+ species. *Catal. Lett.* **1998**, *52*, 103–108. [CrossRef]
32. Chen, H.Y.; Wei, Z.H.; Kollar, M.; Gao, F.; Wang, Y.L.; Szanyi, J.; Peden, C.H.F. NO oxidation on zeolite supported Cu catalysts: Formation and reactivity of surface nitrates. *Catal. Today* **2016**, *267*, 17–27. [CrossRef]
33. Ahrens, M.; Marie, O.; Bazin, P.; Daturi, M. Fe-H-BEA and Fe-H-ZSM-5 for NO2 removal from ambient air—A detailed in situ and operando FTIR study revealing an unexpected positive water-effect. *J. Catal.* **2010**, *271*, 1–11. [CrossRef]
34. Auvray, X.; Olsson, L. Stability and activity of Pd-, Pt- and Pd-Pt catalysts supported on alumina for NO oxidation. *Appl. Catal. B Environ.* **2015**, *168*, 342–352. [CrossRef]
35. Mihai, O.; Trandafilovic, L.; Wentworth, T.; Torres, F.F.; Olsson, L. The Effect of Si/Al Ratio for Pd/BEA and Pd/SSZ-13 Used as Passive NOx Adsorbers. *Top. Catal.* **2018**, *61*, 2007–2020. [CrossRef]
36. Sadokhina, N.; Smedler, G.; Nylén, U.; Olofsson, M.; Olsson, L. The influence of gas composition on Pd-based catalyst activity in methane oxidation—Inhibition and promotion by NO. *Appl. Catal. B Environ.* **2017**, *200*, 351–360. [CrossRef]
37. Sadokhina, N.; Ghasempour, F.; Auvray, X.; Smedler, G.; Nylén, U.; Olofsson, M.; Olsson, L. An Experimental and kinetic modelling study for methane oxidation over Pd-based catalyst: Inhibition by water. *Catal. Lett.* **2017**, *147*, 2360–2371. [CrossRef]
38. Zheng, Y.; Kovarik, L.; Engelhard, M.H.; Wang, Y.; Wang, Y.; Gao, F.; Szanyi, J. Low-Temperature Pd/Zeolite Passive NOx Adsorbers: Structure, Performance, and Adsorption Chemistry. *J. Phys. Chem. C* **2017**, *121*, 15793–15803. [CrossRef]